Project Summary

Future progress in high energy physics depends upon the construction of larger and more powerful particle accelerators. The interior surfaces of these accelerators must be perfectly clean. To reduce the risk of contamination, we must assemble accelerator components with the minimum of human contact. A system of motorized stages and machine vision is an obvious way to maneuver components without human contact, but efforts to use machine vision have been thwarted by the mirror-like surface finish of the vulnerable components.

We are building a machine vision system capable of measuring the position of highly-reflective components. Our system illuminates the components from behind with a uniform field of infrared light. It views the components with stereoscopic cameras that see only infrared light. Modern assembly-room lighting does not contain infrared light, so our cameras do not see reflections off the component surfaces. Instead, we see each component as a dark silhouette. Our stereoscopic silhouette cameras allow us to determine the position and orientation of a component with sufficient precision to bring mating flanges into contact, and to ensure that their bolt holes are perfectly aligned.

In Phase I we built a prototype stereoscopic silhouette camera and infrared backlight. We devised and implemented image-analysis and ray-tracing routines to deduce the location of objects from their silhouettes. We demonstrated that we can measure the position of mirror-finish spheres and cylinders. In Phase II we will build a full-sized system with motorized stages. With the help of our collaborators, we will test our system with actual accelerator components in a working accelerator assembly room. We will expand our software to support all shapes that arise in accelerator construction and we will improve the efficiency of our image analysis so that automated assembly can proceed rapidly.

Our contactless position measurement system has immediate application in all existing accelerator assembly rooms. We expect construction of a new particle accelerator, larger than any that has come before, to begin in the next few years. Construction of this accelerator will require dozens of automated assembly rooms and hundreds of contactless position measurement systems. The growth of the fusion power industry offers another potential market for our system. Fusion plants require regular disassembly and reassembly. They also require that human contact be minimized, not because we want to avoid contaminating the components, but because the components will be radioactive, and will therefore contaminate their human handlers.

Key Words: particle accelerator, machine vision, string assembly, optical alignment, remote assembly, highly reflective components

Summary for Members of Congress: The particle accelerators that support high energy physics research require automated assembly with the minimum of human contact. This project will provide a system of cameras and motorized stages that maneuvers accelerator components into precise alignment without human contact.

Contactless Position Measurement for Highly Reflective Components

Proposal Submission date: April 18, 2023

BAA/FOA Number: DE-FOA-0002991 Phase II Release 2 SBIR
Department of Energy

SBIR Topics FY22 Phase I Release 2
Topic: 30. Radio Frequency Accelerator Technology
Sub-Topic: b. Automation of SRF Cavity String Assembly

Phase II proposal for renewal funding
Phase I Award DE-SC0022581

Lead Institution: Open Source Instruments, Inc.
PI: Kevan Hashemi
Email: Hashemi@opensourceinstruments.com
Address: 135 Beaver Street, Suite 207
Waltham, MA 02452-8424

Table of Contents

Background

From Topic 30.b. “Automation of SRF Cavity String Assembly SRF cavities and other highly reflective metallic components are assembled together in a cleanroom environment. At present the largest impact on the quality of the assembly is the human factor. In order to minimize this impact and also to decrease touch labor and cost, vision-assisted assembly technology is of great interest. Full digitalization of the assembly area, contactless measurement of the component positions, assisted positioning and alignment are some of the steps that could be implemented. The ultimate goal is to develop a contactless technology to reconstruct the pose of highly reflective metallic components to enable a machine assisted assembly of SRF components in a cleanroom environment.”

Future progress in high energy physics depends upon the construction of larger and more powerful particle accelerators. These accelerators will use strings of Superconducting Radio-Frequency (SRF) cavities to accelerate their particle beams and replace the kinetic energy the beam loses to synchrotron radiation. The interior surfaces of these SRF cavities must be perfectly clean, or else they fail to provide sharp enough resonance at their operating radio frequency. The assembly team measures the performance of each cavity after it has been attached to its string and cooled down within its cryogenic chamber. According to all SRF string assembly groups we have spoken to, approximately one in five cavities fail to resonate adequately because they have been contaminated by some particle or residue. The cavity must then be removed, washed, dried, re-installed, and tested again. This decontamination and reinstallation process takes two weeks.

Tracking Number:GRANT13862200 Funding Opportunity Number:DE-FOA-0002991 Received Date:Apr 15, 2023 06:05:42 PM EDT

Figure 1: Example Clean-Room Environment, Superconducting Radio-Frequency (SRF) Assembly Room at Fermi National Laboratory (FNL). Courtesy of Mattia Parise, FNL.

Significance

All string assembly teams agree that human contact is the main source of cavity contamination. The stage at which contamination is most likely to occur is when a human operator joins two pipe flanges together. The operator must remove the caps from the two flanges, thus exposing the interior of the cavity. The operator must maneuver the two flanges into contact and align their bolt-holes. It is during this maneuvering by human hands that contamination is most likely to take place. Once the two flanges are touching, the cavity interiors are no longer exposed and the risk of contamination has passed. It is hard to determine when a contamination takes place, because the first time the assembly team can check for contamination is when the cavity is installed in its string and cooled to its superconducting temperature. Nevertheless, the string assembly groups we have talked to tell us that an automated system for aligning exposed components would reduce their contamination rate dramatically.

One way to remove the human operator from the flange-maneuvering process is to install a machine vision system and some motorized stages that will maneuver the two flanges into contact. Efforts to apply machine vision to this problem have, however, been thwarted by the mirror-like surface finish of SRF components. When a traditional machine vision system views a mirror-like component, it cannot find the outline of the component because it is confused by bright, distorted images of the surrounding string assembly room and its mirror-like contents.

Tracking Number:GRANT13862200 Funding Opportunity Number:DE-FOA-0002991 Received Date:Apr 15, 2023 06:05:42 PM EDT

The solution we propose is to illuminate the highly-reflecting components from behind to obtain silhouette images devoid of reflections near their outlines. The components will appear as black shapes, and we can measure their position by triangulation with two Silhouette Cameras (SCAMs). We place a backlight that shines with uniform illumination behind two components that must be maneuvered together. The backlight shines with infrared light and the SCAMs are equipped with infrared-only filters. By viewing the components in infrared light, we eliminate the reflected views of the assembly room that would otherwise be visible on every surface of the components. These reflections are generated by the overhead lights of the assembly room, which are invariably LED or fluorescent bulbs, neither of which emit infrared light.

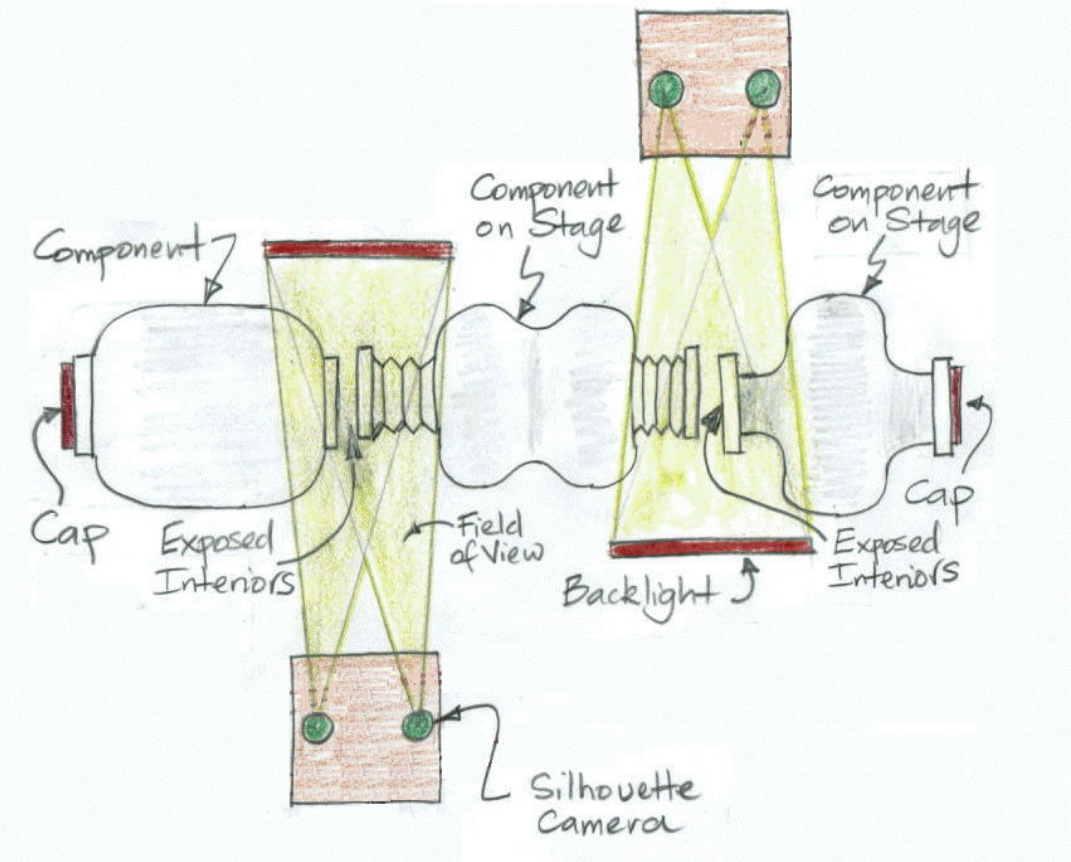

Figure 2: Sketch of Two Contactless Position Measurement Systems (CPMS) Cooperating to Align Three SRF Cavity Components.

Our Contactless Position Measurement System (CPMS) will measure the position of two highly-reflective components and maneuver them into position with motorized stages. In the case of two flanges, the human operator removes the covers from two flanges and exits the clean room. The CPMS brings the flanges into contact and aligns their bolt-holes. With no human present, the risk of contamination while maneuvering is greatly reduced. When the flanges are in contact and perfectly aligned, the human operator returns. The operator inserts bolts and fastens the flanges together. Any contamination shed by

Tracking Number:GRANT13862200 Funding Opportunity Number:DE-FOA-0002991 Received Date:Apr 15, 2023 06:05:42 PM EDT

the human operator during the fastening will be shed on the exterior surfaces of the cavities, which do not take part in the cavity resonance.

The CPMS has immediate application in string assembly rooms. Our collaborators at Fermi National Laboratory (FNL) have been studying the problem of automated assembly in their own SRF cavity facility for several years [12]. Over the next decade we expect the demand for SRF cavities to expand rapidly. The future of High Energy Physics (HEP) research depends upon larger and more powerful particle colliders. Today's Large Hadronic Collider (LHC) provides collisions at 14 TeV. Sixteen SRF cavities are sufficient to overcome the losses due to synchrotron radiation in the LHC. The proposed Future Circular Collider (FCC) will provide collisions at 100 TeV. Synchrotron radiation increases as the fourth power of the collision energy. At 100 TeV, the LHC would need forty thousand SRF cavities. The FCC will be four times the diameter of the LHC, thus reducing the acceleration of the particles by a factor of four. Synchrotron radiation increases as the second power of acceleration, so this quadrupling of diameter reduces the FCC synchrotron radiation by a factor of sixteen. Combining these two effects, we estimate that the FCC will need roughly twenty-five hundred SRF cavities to overcome its synchrotron radiation losses. There will be improvements in the design of the cavities, but the fact remains that the FCC will require one hundred times as many cavities as the LHC.

The CPMS has a longer-term application in the repair and maintenance of fusion reactors. No power-producing fusion reactors exist today, but there are many prototype reactors being built and tested. All these prototypes are built out of highly-reflective metallic components. Any components near the fusion plasma are irradiated by neutrons and gamma rays. These neutrons react with iron and cobalt nuclei to create radioactive isotopes. The time that human operators can spend near the components is limited. The half-life of the iron-55 and cobalt-60 activation is several years, so there is no point in waiting for the components to become less radioactive before repairing them. Maintenance of irradiated components takes place in separate rooms called test cells. By turning one entire wall of a test cell into an infrared backlight and setting up a dozen cameras on the other wall, we could direct motorized stages and robots as they repair and re-assemble the radioactive components.

Phase I Work Done

So far in our Phase I work, we have designed and built a half-sized contactless position measurement system (CPMS), designed the optics for our silhouette cameras (SCAMs), developed the image analysis software required to locate compound reflecting objects in its field of view, and obtained 50-µm measurement precision with the half-sized CPMS. We have been recording our work in our Development Log [1]. We summarized our work in our Interim Research Performance Report [2].

Tracking Number:GRANT13862200 Funding Opportunity Number:DE-FOA-0002991 Received Date:Apr 15, 2023 06:05:42 PM EDT

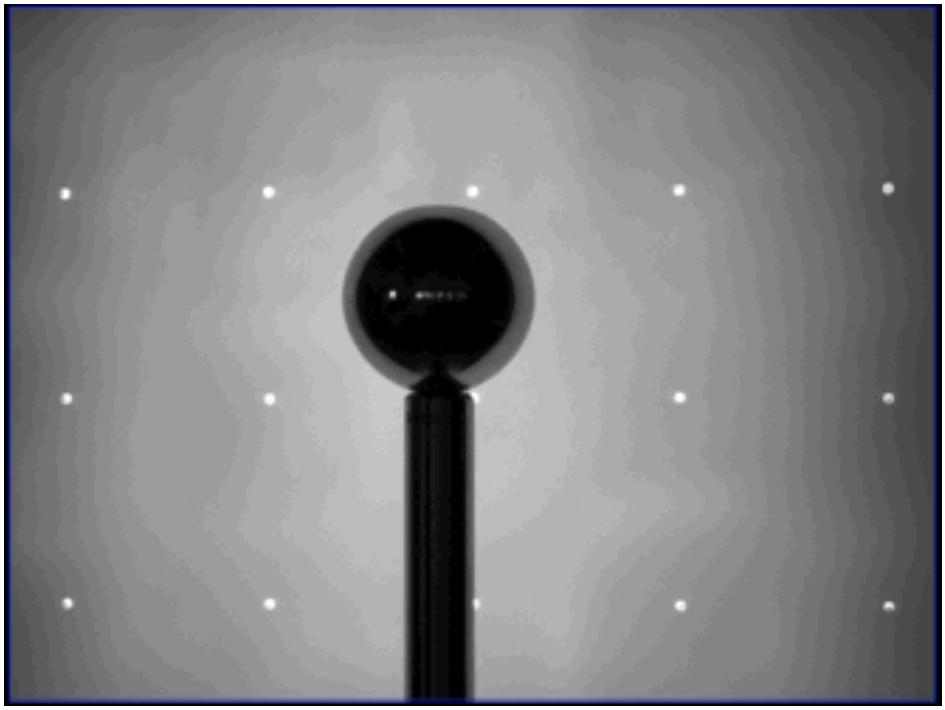

Figure 3: Post and Sphere Pressed Up Against Backlight. Bright spots are light-emitting diodes behind the backlight diffuser. We see reflection of the backlight around the perimeter of the sphere. We see reflections of windows at the center of the sphere.

A full-size CPMS would be roughly 180 cm from SCAMs to backlight. In our half-size CPMS we have 90 cm from SCAMs to backlight. Our backlight consists of an array of infrared Light-Emitting Diodes (LEDs) on a 50-mm grid. A pane of white diffusing glass is mounted 50 mm in front of the LEDs. When we view this backlight, we see regular bright spots corresponding to the location of each LED. These bright spots have no effect upon silhouette analysis, as can be deduced from the white-glass residuals in Figure 6. The rest of the backlight is a slowly-varying field of infrared light. We equipped our half-sized CPMS with a backlight 20 cm square, but our backlight is designed in such a way that it may be tiled with other backlights to illuminate a 1-m square pane of white glass to make a 1-m square backlight.

We used micrometer stages to move highly-reflecting posts and spheres across the field of view of our SCAMs. We developed image analysis and ray tracing software that allows us to deduce the location and orientation of a component using one or two silhouette images. We used the linearity of our measurements with stage position to demonstrate the performance of our backlight.

Tracking Number:GRANT13862200 Funding Opportunity Number:DE-FOA-0002991 Received Date:Apr 15, 2023 06:05:42 PM EDT

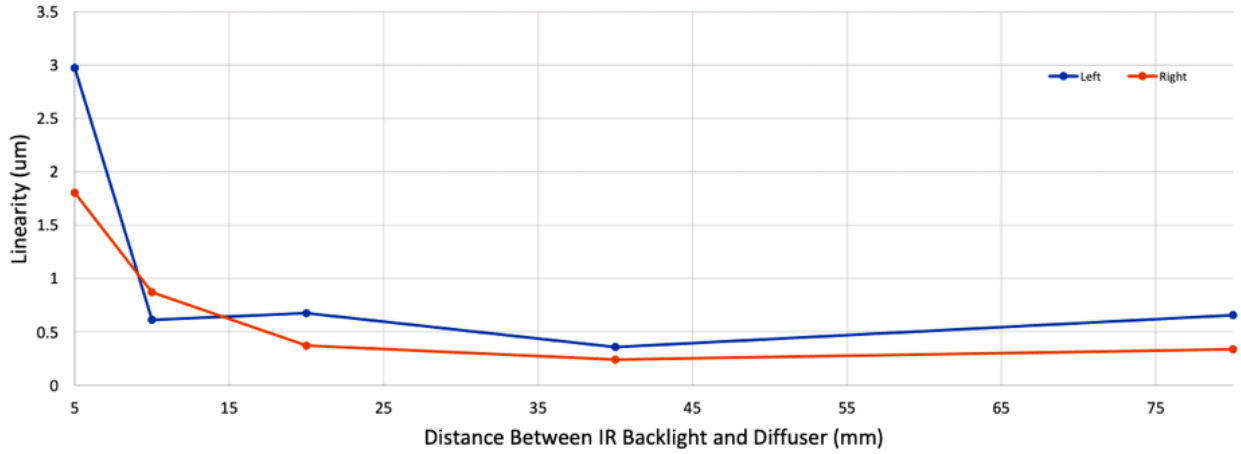

Figure 4: Linearity of Silhouette Edge Tracking versus Backlight Spacing. We vary the spacing between the LED array and a ground glass diffuser. For each spacing we move a post with our manual stage, fit a straight line to image position versus stage position, and take the standard deviation of the residuals as our measure of linearity.

We tried a variety of commercially-made and compound lenses in our half-sized CPMS, but in the end we found that the best-performing optics were a 2.7-mm aperture pressed up against a single plano-convex lens. These optics approximate a pin-hole camera. They provide ample depth of field and linear projection onto our image sensors. The sensors themselves are CCDs (Charge Coupled Devices). We chose CCD sensors in preference to CMOS (Complementary Metal Oxide Semiconductor) sensors because we know they provide images of sufficient quality, and we did not want to complicate our development by testing new sensors. We flash our backlight and read out our image sensors with our Long-Wire Data Acquisition (LWDAQ) hardware [13] and software [14]. We first developed the LWDAQ twenty years ago for the alignment system of the ATLAS end-cap muon spectrometer [11]. The LWDAQ allows us to clear the image sensors, flash the backlight, and read out both images synchronously. The readout takes place pixel by pixel, so as to preserve the exact geometry of the projected silhouettes.

We tried edge-finding and outline-tracing as a way to analyze silhouette images in our initial studies. We have used edge-finding successfully in the past to find wires and ellipses in x-ray and optical images [4, 6, 7]. Our initial studies of the linearity of the silhouette measurement we performed with an edge-finding algorithm applied to the silhouette of a highly-reflecting post. We used these studies to choose the diffuser for our backlight. Residuals on the image sensor with white glass were approximately 1 μm rms, or roughly 50 μm rms in the post position at range 1 m.

Tracking Number:GRANT13862200 Funding Opportunity Number:DE-FOA-0002991 Received Date:Apr 15, 2023 06:05:42 PM EDT

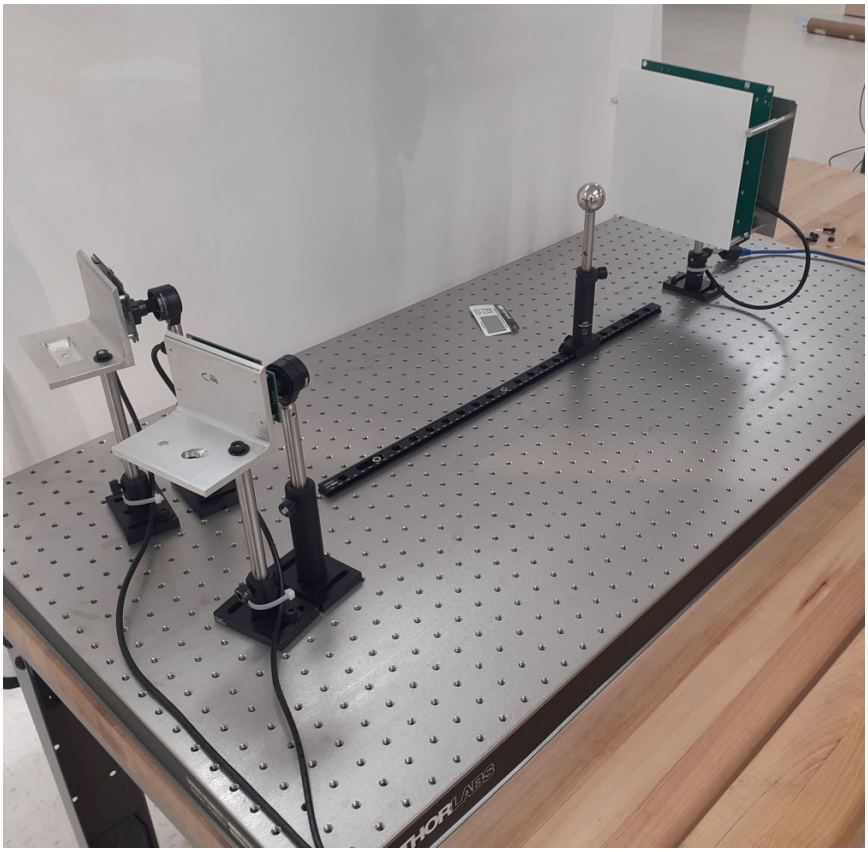

Figure 5: Half-Size CPMS Configured to Measure Depth of Field. We have 90 cm from the SCAMs to the backlight. A sphere and post move from the backlight to cameras.

When it came to the complex shapes that the CPMS must locate, outline-tracing proved to be cumbersome and unreliable. We developed a more versatile analysis, one that can accommodate complex components with no fundamental changes in the way it operates. In all CPMS applications, we will have drawings of every component, and every component will be machined with high precision. Our analysis constructs a computer model of each component by combining simple shapes like spheres and cylinders until the combination matches the actual component. When we measure the location of a component, we start by giving our modeled component a location that is close to that of the actual component. We project the modeled component onto the image sensor of our camera and obtain a modeled silhouette. The modeled silhouette and the actual silhouette are not aligned. We proceed to adjust the position of the modeled component until we align the modeled and actual silhouettes as best we can. The final position of the modeled component is our measurement of the position of the actual component.

Tracking Number:GRANT13862200 Funding Opportunity Number:DE-FOA-0002991 Received Date:Apr 15, 2023 06:05:42 PM EDT

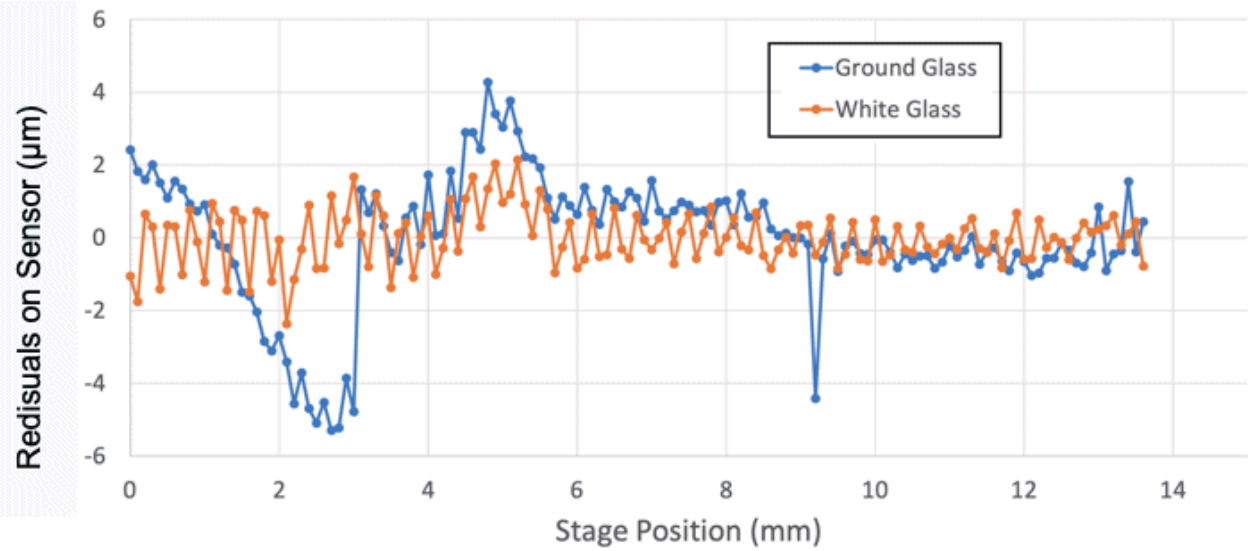

Figure 6: Linearity of Image Position for Two Types of Diffusing Glass. Image magnification is 1/44. We plot residuals from a straight line fit of edge position on the image sensor versus stage position. The cyclic component of the residual has period one half of the image sensor pixel.

The only analysis we perform on the actual silhouette image is to classify every pixel as either “silhouette” or “backlight”.

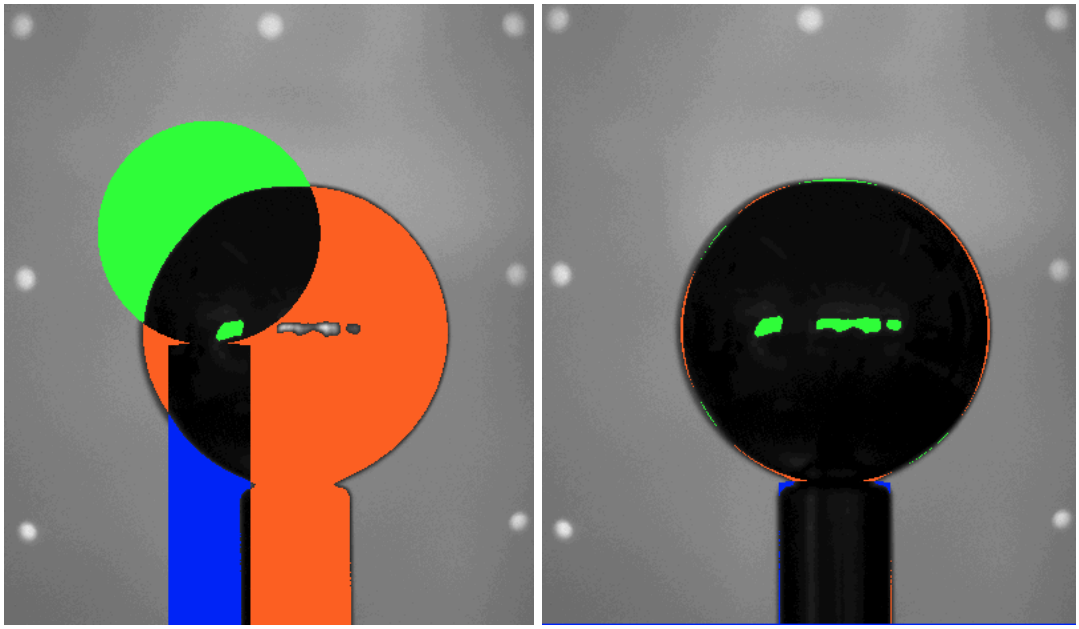

Figure 7: A Classified Silhouette Image with Model Projection Overlayed and Disagreement Color-Coded. Left: Before fitting. Right: After fitting.

In Figure 7 we see the comparison of an actual and modeled silhouette color-coded in the overlay of one of our gray-scale SCAM images. Any pixel in which the modeled silhouette and actual silhouette agree we leave as a gray-scale pixel. Any pixel that is part of the actual silhouette, but not part of the modeled

Tracking Number:GRANT13862200 Funding Opportunity Number:DE-FOA-0002991 Received Date:Apr 15, 2023 06:05:42 PM EDT

silhouette we mark in orange. Any pixel that is part of the modeled silhouette, but not part of the actual silhouette, we mark in blue or green. Green is the modeled sphere and blue is the modeled cylinder. The simplest way to obtain the disagreement between the modeled and actual silhouettes is to count the colored pixels.

In the center of the sphere, we see reflections of our sunlight windows. It turns out that these reflections do not disturb our analysis. As we move the modeled component around, the reflections cause a constant offset to the disagreement between the two images. We can tolerate reflections, so long as they are far from the edges of the silhouette. Figure 8 shows how the number of disagreement pixels varies as we offset modeled component position in the two directions perpendicular to the camera axis. Our fitting algorithm arrives at a minimum with precision 50 µm rms, and we can even adjust the model position manually to minimize the disagreement by looking at the colored pixels in the image overlay, and so obtain the same precision of 50 µm rms over ten attempts from a random starting position.

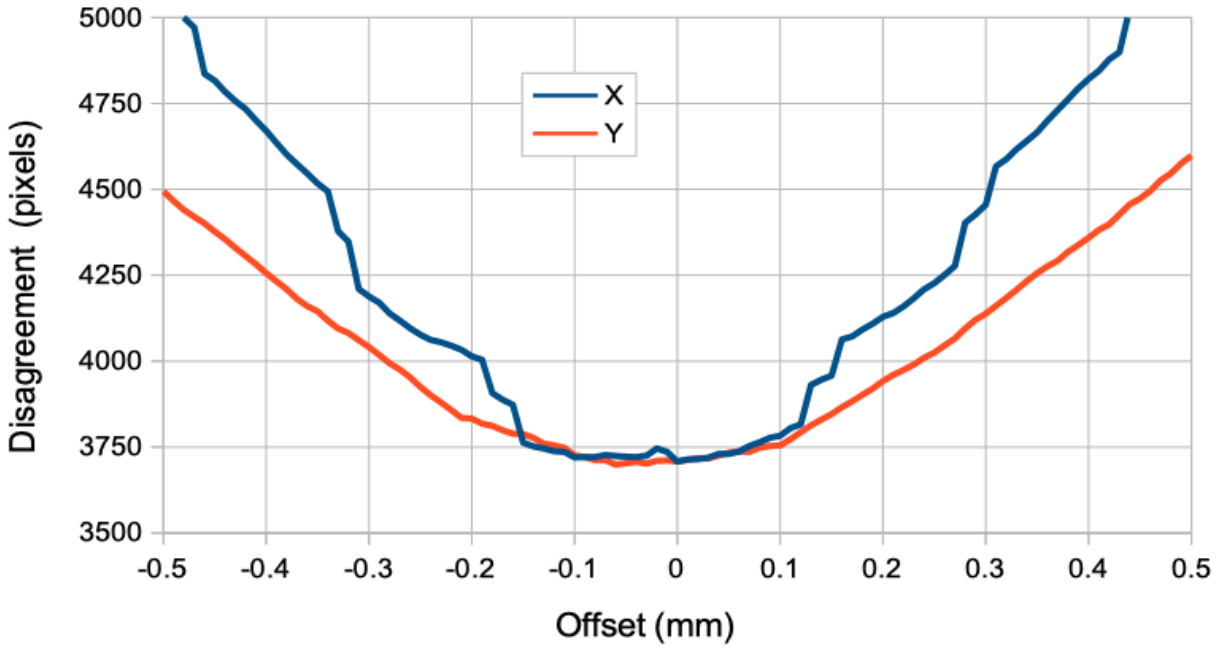

Figure 8: Disagreement (pixels) versus Offset (mm) in X and Y For Silhouette Analysis. Object is a vertical post and sphere at range 52 cm.

We mounted components on micrometer stages to measure precision and resolution of our position measurement. We mounted components on an optical rail to explore dynamic range and depth of field. Because we know the dimensions of the components we will be locating, we can, in principle, deduce the position of the object using only one camera silhouette. With only one camera looking at a combined sphere and post object, our precision is 50 µm in the directions perpendicular to the camera axis, and 500 µm along the axis. With two cameras whose axes are separated by fourteen degrees, our precision along the axes improves to 150 µm. Depth of field in our half-sized system is limited by the size of the backlight. Both cameras look straight at the backlight. As we move an object from range 60 cm to 90 cm, it remains in view of both SCAMs. If we move an object to range 40 cm in front of one of the SCAMs, it is

Tracking Number:GRANT13862200 Funding Opportunity Number:DE-FOA-0002991 Received Date:Apr 15, 2023 06:05:42 PM EDT

still in sharp focus. In a full-sized CPMS with a 1-m square backlight, we expect to have depth of field 80 cm to 180 cm with objects in view of both cameras.

Phase I Work Remaining

At the time of writing, we still have three months remaining in our Phase I grant period. Although we have answered the fundamental questions we set out to answer in Phase I, we have several further goals to accomplish.

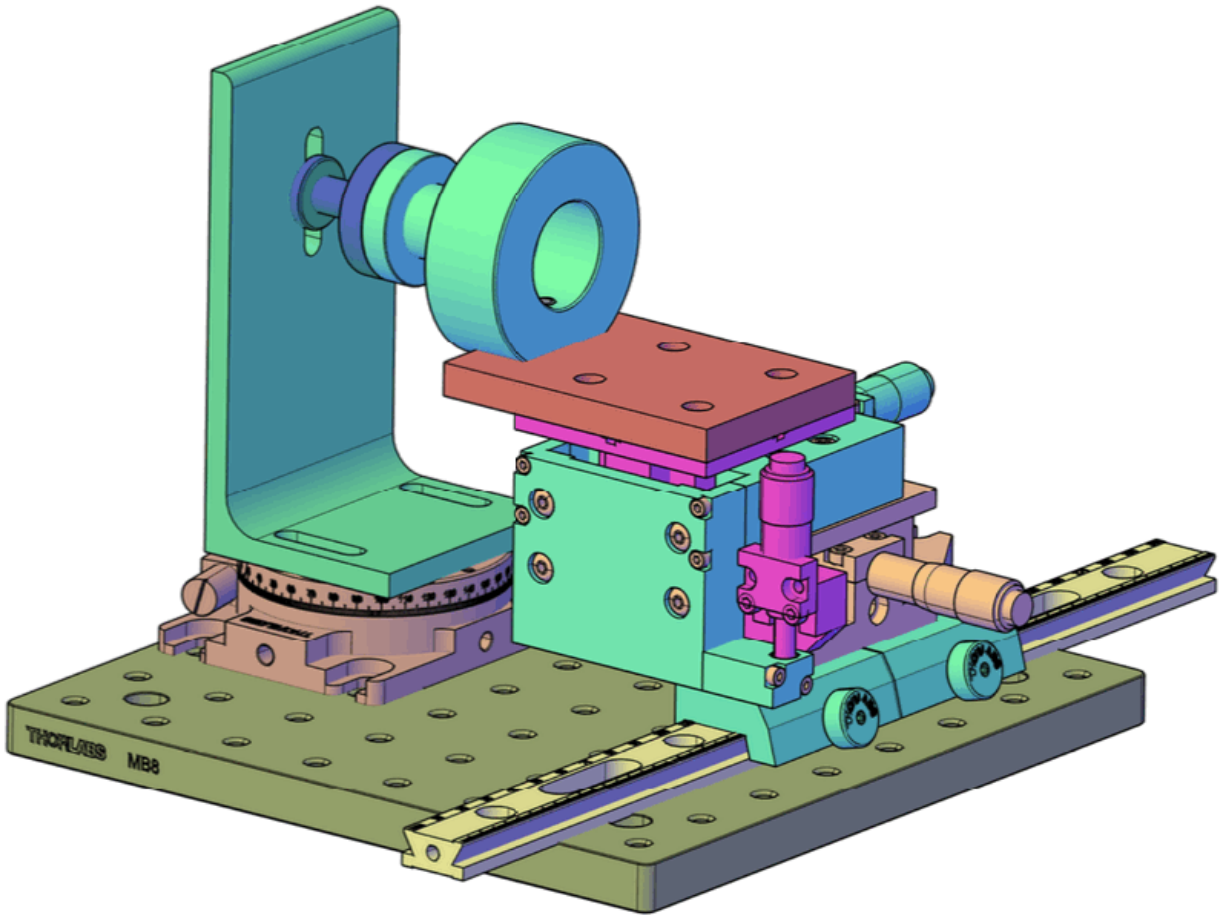

Figure 9: Solid Model of SRF Cavity Flange Replica Mounted on Rotation and Translation Stages. All these pieces exist, either machined for us out of stainless steel, or purchased from a vendor.

The disagreement function our analysis uses to align our modeled component with our actual component is an integer count of disagreement pixels. As we can see in Figure 8, this function is poorly-behaved. It provides us with no definite minimum, and it is not smooth. This poor behavior is the result of our binary classification of pixels as either in agreement or out of agreement. A graduated scale of agreement will provide a smoother disagreement function, but remains to be implemented. Another

Tracking Number:GRANT13862200 Funding Opportunity Number:DE-FOA-0002991 Received Date:Apr 15, 2023 06:05:42 PM EDT

weakness of our existing analysis is its execution time: one measurement takes one minute. We have several ideas for accelerating the analysis, but these ideas remain to be implemented. Because the analysis is slow, systematic tests of linearity and precision have been impractical. At the time of writing, we have three months of technical work left to do in Phase I. We have hired an apprentice computer programmer, who will spend the next three months working on accelerating the analysis. We are hiring an undergraduate student for the summer to perform systematic measurements of linearity and precision with the accelerated analysis and our manual micrometer stages.

Another study we will perform in the final months of our Phase I work is to measure the relative positions of two replica flanges taken from a model of an SRF assembly provided to us by our collaborators at Fermi National Laboratory. We have these pieces in hand, along with a three-axis translation stage and rotation stage as shown in Figure 9. We will model both flanges as a combination of cylinders, and measure their position and orientation as we translate and rotate them.

One alignment question we have not yet addressed is the problem of aligning bolt-holes. So far, our analysis provides a means for bringing two flanges into flush contact, with their cylindrical axes coincident, but it does not provide a way to rotate a flange about its cylindrical axis until its bolt holes align. We will try out some preliminary ideas for how to measure cylindrical rotation before our Phase I work ends, such as attaching a pin to each flange, or attaching a battery-powered infrared light source. But the main work we anticipate for this problem will be forming a relationship with the designers of the components whereby they will be willing to modify their drawings to include fixtures for mounting our alignment fiducials. We plan to dedicate far more time to this question in Phase II.

Although we have some refinement of our analysis, and we have yet to explore the fundamental limits of the accuracy of the CPMS, we are confident that the CPMS will provide the accuracy required for aligning the highly-reflecting components.

Phase II Work, Overview

In Phase II of our work, we will focus on four objectives. First, we will solve the problem of measuring the orientation of radially-symmetric components about their axis of symmetry so that their bolt-holes may be aligned. Second, we will solve the problem of absolute calibration of our SCAMs and their mounting plate so that we can obtain absolute measurements of the separation of components as the CPMS maneuvers them together. Third, we will build a full-size, motorized CPMS and test it with actual SRF cavity components in a real string assembly facility. Fourth, we will study the possible adaptation of the CPMS for application in the maintenance of fusion reactors. In our pursuit of the first three objectives, we will work closely with our collaborators at Fermi National Laboratory (FNL), who we are subcontracting to set up and test our prototypes in their own assembly room.

Tracking Number:GRANT13862200 Funding Opportunity Number:DE-FOA-0002991 Received Date:Apr 15, 2023 06:05:42 PM EDT

Bolt-Hole Alignment

When we connect two steel flanges together, the most common way to fasten them securely in place is with bolts. There might be six bolts arranged around each flange. They may be threaded, or they may both be clearance holes. We must align the correct holes with one another. Indeed, it is the alignment of bolt-holes that dictates the required accuracy of the CPMS. With a half-millimeter clearance around a bolt, we must align the holes to within two hundred microns. In order to provide this alignment, the stage upon which one of the components is mounted must provide not only three axes of translation, but also three axes of rotation. Setting aside the question of how to provide these three axes of rotation with stages suitable for a clean room environment, let us consider the problem of measuring the orientation of a flange about its cylindrical axis.

As the two flanges are brought together, we have no hope of seeing their bolt holes in our silhouette images. At some point, we will no longer see the gap between them. But our component-modeling analysis will still be able to deduce the distance between them, and their orientations about all axes save for the cylindrical axis. In order to measure the rotation about the cylindrical axis, we must modify the component in some way to break its radial symmetry.

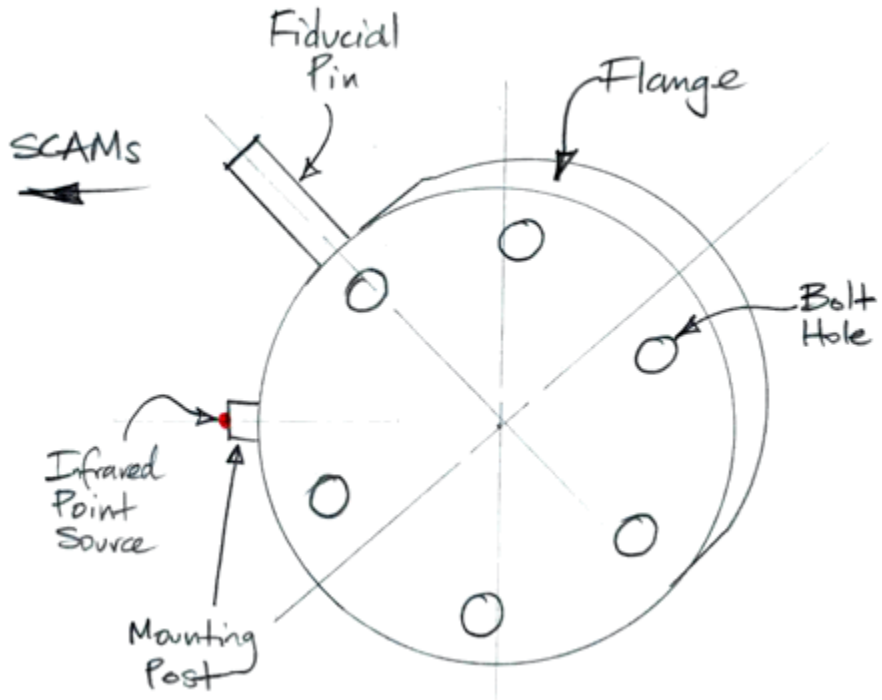

Figure 10: Forty-Five Degree Fiducial Pin and Battery-Powered Infrared Point Source for Bolt Hole Alignment.

Suppose each flange provides a 2-mm deep hole on the top side. We place a 52-mm pin in this hole, so that it protrudes by 50 mm above the flange. The view of our CPMS is near-horizontal, so we will be able to measure the altitude of the top of the pin with accuracy 50 μm rms. As the flange rotates about its

Tracking Number:GRANT13862200 Funding Opportunity Number:DE-FOA-0002991 Received Date:Apr 15, 2023 06:05:42 PM EDT

cylindrical axis, the altitude of the top of the pin will vary. But when the pin is vertical, its altitude varies only as the cosine of rotation. A 10-mrad rotation from vertical will drop the altitude by only 2 μm, which is too small for us to measure.

We have two ideas for how to solve the bolt-hole alignment problem. One is to attach the pin to the flange at forty-five degrees to the vertical, and make the pin long enough that it is visible above the silhouette of the flange itself. Now we have the altitude of the pin varying as the cosine of forty-five degrees.

Another idea is to place a battery-powered infrared point source half-way up the flange, so that it is viewed nearly head-on by the SCAMs. As we saw in Phase I with reflections at the center of a silhouette, this point of light will not disrupt our silhouette analysis. We will be able to locate the spot within the silhouette with a separate spot-finding routine, such as we use with our BCAM (Boston CCD Angle Monitor) images [4]. Our spot-finding routines are well-established and capable of avoiding reflections by examining the shape of a spot and counting the number of pixels it contains. The position of the light source is now a strong function of the flange rotation.

The pin would have to be at least half the diameter of the flange. The hole in which it sits will have to be tight enough and deep enough to ensure that the tip of the pin is located with accuracy of one or two hundred microns. The infra-red light could be smaller, equipped with a short pin at the base. The light itself would have to be centered on the mounting pin axis with precision 100 μm so the operator does not have to worry about the orientation of the light when they place the light in its socket in the flange.

Both of these ideas seem promising to us, but both require integration of the fiducial mount to the drawing of the component. Both types of fiducial are accommodated by our existing library of image analysis algorithms. Both types will need to be built and tested.

Absolute Calibration

So far we have studied the precision and linearity of the CPMS, but we have not attempted to perform an absolute measurement of component position or orientation. By “absolute measurement” we mean the measurement of position and orientation in a known coordinate system, not merely the measurement of the distance a component has moved. Ultimately, we are interested only in the relative position of the two components we wish to align. In order to obtain their relative positions in the directions parallel to the SCAM axes, however, we must measure their absolute positions in the directions perpendicular to the SCAM axes.

Any measurement of component range using only one silhouette suffers from a systematic error generated by our intensity threshold. Pixels darker than the threshold we classify as within the silhouette. All others are outside the silhouette. Because the edges of the silhouette are slightly blurred, increasing the threshold decreases the width of the silhouette, which in turn suggests that the object is farther away. Similarly, increasing the exposure time decreases the width of the silhouette, leading us to conclude that the object is farther away.

Tracking Number:GRANT13862200 Funding Opportunity Number:DE-FOA-0002991 Received Date:Apr 15, 2023 06:05:42 PM EDT

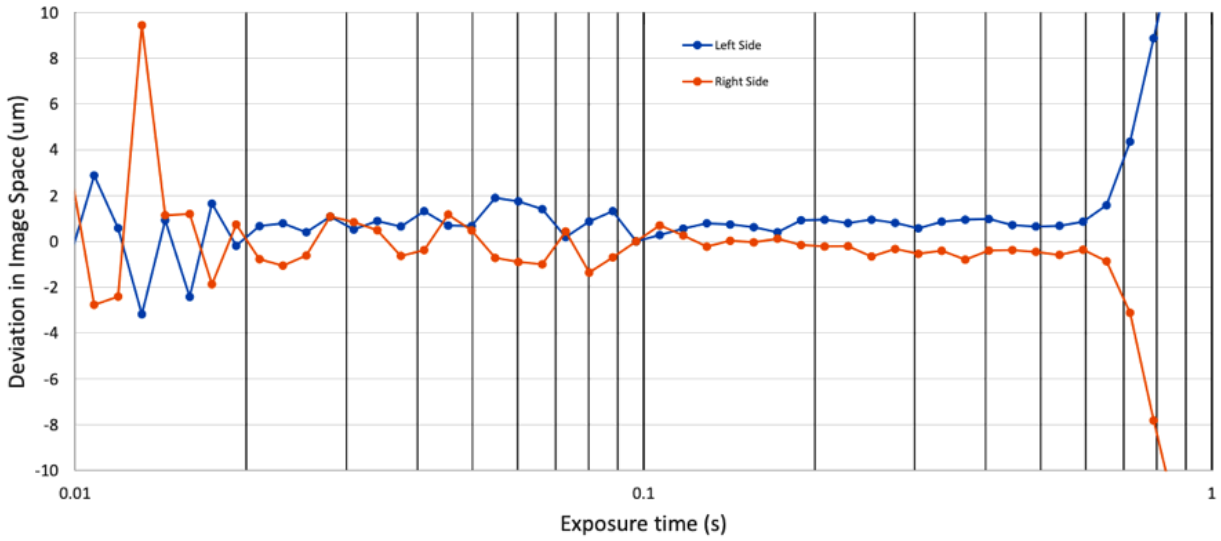

Figure 11: Deviation of Left and Right Edges of Post versus Exposure Time. Left and right edges move towards one another as the backlight becomes brighter.

In order to measure range with accuracy sufficient to align bolt holes, we must use two silhouette images taken by two separate cameras and deduce the range by triangulation. One of the fundamental requirements of triangulation is that we know the length of the base of our triangle. Another is that we know the angle subtended by this base at the triangulation point. In our experiments so far, we have measured the precision we could obtain by triangulation, but in order to measure the relative ranges of two objects accurately, we must calibrate our two SCAMs and the plate upon which we mount them.

We will construct our stereoscopic CPMS camera by mounting two SCAMs on a stiff aluminum plate. We orient the SCAMS so that their fields of view intersect where we expect to place our components. In the case of the full-sized CPMS, we estimate that this range will be approximately 1.2 m. We mount the SCAMs the same way we mount BCAMs [3]. The SCAM will look, from the outside, much like a BCAM. Underneath it has a cone, slot, and flat designed to sit on three steel balls each one quarter of an inch in diameter. The three balls define a mount coordinate system for each SCAM. On the front face, the SCAM presents a lens and infrared-only filter. On the back it presents a socket for a cable that provides power, control, and readout. The plate will provide the two sets of mounting balls for its two SCAMs.

Tracking Number:GRANT13862200 Funding Opportunity Number:DE-FOA-0002991 Received Date:Apr 15, 2023 06:05:42 PM EDT

Figure 12: The N-BCAM Used in the ATLAS End-Cap Muon Alignment System. Left: Lens and laser openings visible. Right: Cone, slot, and flat kinematic mounting depressions. The SCAM will look much the same, but without the lasers.

We have experience calibrating metrology devices [8, 9, 10]. We propose to calibrate our CPMS with the help of a coordinate measurement arm. We provide the camera mounting plate with three additional balls that define a CPMS coordinate system. We mount the CPMS on an optical table along with a coordinate measuring arm and a selection of reference objects such as spheres, posts, and cubes. We place our backlight behind the objects. We take silhouette images of all the objects. We model the SCAMs as pinhole cameras, just as we model BCAMs as pinhole cameras. Each camera may be defined by seven parameters, so long as we permit ourselves to assume that the image sensor is perpendicular to the camera axis. These parameters are: the three-dimensional position of the lens center, the three-dimensional position of the image sensor center, and the rotation of the image sensor about the camera axis. Together, these seven values are the calibration constants of an SCAM. We assume nominal values for the calibration constants and proceed to adjust them with a minimization algorithm until the disagreement between our reference object silhouette images is minimized. With this absolute calibration, we expect our CPMS to provide absolute measurements of position with accuracy 50 μm rms at ranges 80 cm to 180 cm. In order to support our calibration of CPMS cameras, we will purchase a CMM arm during our Phase II work.

Full-Size Prototypes

In the first year of our Phase II work, we will build two identical Version-One (V1) prototype CPMSs. The V1 will be designed for use in SRF cavity assembly. We will work with our collaborators at FNL to draft the specification of the V1 before we build it. The V1 will be equipped with a six-axis manual stage to maneuver one of two components, and served by a user interface that instructs the operator on how to

manipulate the stages so as to move the two components into alignment. We will ship the first V1 to FNL, where our collaborators at that institution will set up the CPMS in their SRF cavity assembly facility. They will exercise the CPMS with real SRF cavity components. The second V1 prototype we will keep at our own facility, where we will use it to duplicate the problems discovered by the group at FNL. After several weeks of testing, we will work with the FNL group on the design of the next prototype.

In the second year of our Phase II work, we will construct a pair of V2 prototypes. The V2 prototype will be fully-calibrated by our coordinate measuring machine so that it provides the absolute position of components in the coordinate system defined by its reference plate. The V2 will be equipped with a six-axis motorized stage to move one of two components into position automatically under control of our CPMS software. We will ship the first V2 to FNL, keep the other one ourselves, and work with FNL for several weeks to exercise the V2. We will deem the V2 successful if it is capable of aligning bolt-holes on two flanges we place in random starting positions. The success of the V2 prototype in aligning flanges will be the most important milestone of our Phase II work.

Fusion Application

Private investors and the Department of Energy are taking a keen interest in the development of fusion power. Fusion reactors may or may not start contributing to electricity generation in the next ten years, a growing number of prototype fusion reactors are being built. These prototypes sustain fusion reactions, even if they are not yet capable of delivering more power than they consume. Nuclear fusion produces high-energy neutrons. The deuterium-tritium reaction, for example, produces 14-MeV neutrons. These neutrons leave the plasma immediately. They pass without hindrance through the containing magnetic field and strike the walls of the reactor, where they generate heat. The heat is welcome, but the other effects of the neutrons are not. High-energy neutrons shatter the crystalline structure of metals, eventually leading to embrittlement and loss of strength. As a result, fusion reactor components require frequent maintenance and replacement.

Any component that requires maintenance due to embrittlement will be radioactive. Neutrons convert iron-56 into iron-55 and cobalt-59 into cobalt-60. The former emits x-rays and the latter gamma-rays. The neighborhood of the reactor is particularly dangerous, so components that can be removed are transported by robot to chambers where the only source of radiation is the component itself.

In a study of the DEMO fusion reactor [5], the ionizing dose rate outside the radiation shield during shut-down was at least 0.01 Gy/hr. If so, the dose rate at the surface of an embrittled component would also be 0.01 Gy/hr or greater. Given that the maximum annual dose permitted for a human operator per year in the US is 0.05 Gy [15], we see that human operators may be permitted only five hours per year handling such objects, or a few minutes per day. Everyone we spoke to in the fusion reactor field agreed that robotic repair and maintenance was a high priority for them. But when it comes to guiding robots to align parts during repair, they face the same problem as SRF cavity construction. Most of their components are made of shiny stainless steel.

Once a damaged component has been taken to a maintenance chamber, it is in an ideal location for application of a CPMS for remote repair. We could equip one entire wall of a maintenance chamber with

a backlight, and the opposite wall with half a dozen SCAMs, and so provide the absolute position of flanges and other protruding features as well as the position of bolts and fixtures held in the jaws of a robot. This CPMS would be much larger than the ones we plan for SRF cavity assembly. During Phase II we will attempt to form a collaboration with a fusion reactor group with the objective of designing a remote repair system for fusion reactor maintenance.

Milestones

During Phase II we aim to meet the following milestones. For each milestone, we specify whether Open Source Instruments (OSI) or Fermi National Laboratory (FNL) has primary responsibility for accomplishing the task.

Milestone Zero, Beginning of Month Zero: Receive funding for SBIR Phase II. (OSI)

Milestone One, End of Month Two: Complete design of V1 CPMS prototype. (OSI)

Milestone Two, End of Month Eight: Ship V1 CPMS prototype to FNL. (OSI)

Milestone Three, End of Month Ten: Set up a two-meter calibration stand equipped with a coordinate measuring arm. (OSI)

Milestone Four, End of Month Eleven: Complete testing of V1 CPMS, prepare report on performance of the V1 CPMS, make recommendations for the design of the V2 CPMS. (FNL)

Milestone Five End of Month Eleven: Successful bolt-hole alignment with manual stages using V1 CPMS. (OSI)

Milestone Six, End of Month Twelve: Absolute calibration of CPMS to 50-μm accuracy from ranges 90 cm to 180 cm. (OSI)

Milestone Seven, End of Month Fourteen: Form a collaboration with a fusion reactor group. (OSI)

Milestone Eight, End of Month Sixteen: Complete design of V2 CPMS prototype. (OSI)

Milestone Nine, End of Month Twenty: Ship V2 prototype to FNL. (OSI)

Milestone Ten, End of Month Twenty-Three: Complete testing of V2 CPMS. Report on success or failure of the V2 in aligning flanges with bolt-holes. (FNL)

Milestone Eleven, End of Month Twenty-Three: Successful bolt-hole alignment with motorized stages using V2 CPMS. (OSI)

Tracking Number:GRANT13862200 Funding Opportunity Number:DE-FOA-0002991 Received Date:Apr 15, 2023 06:05:42 PM EDT

Milestone Twelve, End of Month Twenty-Four: Complete design of V3 CPMS for use in fusion reactor remote repair. (OSI)

Subcontractor

We will be hiring one subcontractor: Fermi National Laboratory (FNL). Their mailing address is:

Fermilab
PO Box 500
Batavia IL 60510-5011
Phone: 630-840-3000

We will be directing approximately $200k of our Phase II funding to FNL to compensate them for three months engineering and technician time in the first year, and another three months engineering and technician time in the second year. Their job will be to test our prototypes and recommend improvements to the design.

Beyond Phase II

At the end of Phase II, our V2 CPMS will be a working prototype remote assembly system for use with SRF cavity components. We will need no further funding to help us develop or market the CPMS to SRF cavity assembly groups. If, at the end of Phase II, we are collaborating with a fusion reactor group on the design of a remote-repair system for fusion reactor components, we will assess whether or not we can proceed with this work using our own research and development budget, or whether we will need additional funding. At that time, we will consult with our Department of Energy program officer to ask their advice on how to proceed.

Facilities and Equipment

Open Source Instruments has its new laboratory and manufacturing facility at 135 Beaver Street, Suite 207, Waltham, MA. Our 2,900 square foot, rented space has an open floor plan. It is well lit with natural and artificial light. There are 11 distinct work stations in the space, which are comprised of a work-bench surface, seating, magnifier lights, computers, and specialized equipment. Open Source Instruments has equipment necessary for electronic design and assembly. Items include:

Three optical breadboards, one mounted on a vibration-absorbing frame
Ten soldering irons at electronic assembly stations
Three complete telemetry systems for testing and programming telemetry devices
Walk-in Faraday canopy for testing telemetry systems
Optical fiber stretcher to heat and taper optical fibers

Oscilloscopes and digital voltmeters
Custom-made silicone curing station for silicone coatings
Cleaning station with hot water, brushes, and compressed air
Vacuum chamber for epoxy encapsulation of telemetry sensors
Motorized rotators for encapsulation curing
Frequency synthesizers and function generators
Photodetectors, fiber light injectors, and cameras
Surface mount reflow oven and manual paste printer
Accelerated aging oven
Inspection optics

The facility is large enough to include space for storing items related to manufacturing, such as electronic components, printed circuit boards, epoxy, manufactured parts ready for sale, Faraday enclosures, and packing materials. There are shelves for disposable items like mixing tips, paper containers, and wipes. The new space is large enough to absorb growth in both projects and people. The Open Source Instruments billing and correspondence address is the same as our laboratory and manufacturing facility. Accounting, invoicing, and bill-payment all take place at 135 Beaver Street, Waltham.

References

[1] CPMS Development Log, https://www.opensourceinstruments.com/CPMS/Development.html
[2] CPMS Interim Report, https://www.opensourceinstruments.com/CPMS/Reports/Interim_12APR23.pdf
[3] BCAM User Manual, http://www.bndhep.net/Devices/BCAM/User_Manual.html
[4] BCAM Instrument, http://www.bndhep.net/Electronics/LWDAQ/Manual.html#BCAM
[5] Shutdown dose-rate assessment during the replacement of in-vessel components for a fusion DEMO reactor, Someya et al, https://doi.org/10.1016/j.fusengdes.2017.02.108
[6] Rasnik Analysis, http://www.bndhep.net/Devices/RASNIK/Analysis.html#Introduction
[7] The WPS Instrument, http://www.bndhep.net/Electronics/LWDAQ/Manual.html#WPS
[8] BCAM Calibration, http://www.bndhep.net/Devices/BCAM/Calibration.pdf.
[9] WPS Calibration, http://www.opensourceinstruments.com/WPS/WPS1/Calibration.html.
[10] BCAM Camera and Source Calibration on a Granite Beam, http://www.opensourceinstruments.com/GMS/BCAM_Calibration/Report.html.
[11] The Optical Alignment System of the ATLAS Muon Spectrometer Endcaps, Amelung et al., http://www.bndhep.net/ATLAS/ECA.pdf
[12] Computer Vision solutions for Robot-assisted technology in SRF assembly at Fermilab, Zorzetti et al, https://www.opensourceinstruments.com/CPMS/Reports/TTC_SRFautomation_SZ.pdf
[13] LWDAQ Hardware, http://www.bndhep.net/Electronics/LWDAQ/LWDAQ.html
[14] LWDAQ Software, http://www.bndhep.net/Electronics/LWDAQ/Manual.html
[15] U.S.NRC Limits, https://www.nrc.gov/reading-rm/doc-collections/cfr/part020/part020-1201.html